Chemical Physics 75 (1983) 305–322
North-Holland Publishing Company

# NICKEL PORPHYRIN PHOTOPHYSICS AND PHOTOCHEMISTRY. A PICOSECOND INVESTIGATION OF LIGAND BINDING AND RELEASE IN THE EXCITED STATE

Dongho KIM, Christine KIRMAIER and Dewey HOLTEN
*Department of Chemistry, Washington University, St. Louis, Missouri 63130, USA*

Received 4 October 1982

The photophysical behavior and some photochemical processes for nickel(II) porphyrins have been examined with picosecond transient absorption techniques. Detailed results are reported for Ni-octaethylporphyrin (NiOEP) and Ni-protoporphyrin IX dimethylester (NiPPDME) in toluene, pyridine and piperidine. Excitation flashes at six wavelengths between 355 and 532 nm have been employed. In toluene, rapid (≤ 15 ps) radiationless decay occurs via several pathways to the low-lying $^3B_{1g}$ excited state. In the basic solvents pyridine and piperidine, excited states with nickel $^1A_{1g}(d_{z^2})$ character have a tendency to release ligands bound to the metal. Excited states with nickel $^1B_{1g}$ or $^3B_{1g}$ ($d_{z^2}, d_{x^2-y^2}$) character on the other hand, have an affinity for basic ligands which rapidly bind to the metal. The competition between radiationless decay, ligand binding and ligand release depends on the nickel porphyrin, solvent and excitation wavelength. A set of "rules" has been developed that gives a consistent view of all of our results and those of previous investigators. These results may be helpful in understanding photoprocesses in other transition-metal porphyrins, including hemes, which have particular biological significance.

## 1 Introduction

Metalloporphyrins are ubiquitous in nature. Their roles are crucial in a variety of biological transformations [1]. Iron porphyrins (hemes) function as the active sites in hemoglobin and myoglobin to reversibly bind oxygen and carbon monoxide. They also act as redox catalysts in peroxidase, catalyase and cytochromes. The magnesium porphyrins, chlorophyll and bacteriochlorophyll, serve as light-harvesting and electron-transfer pigments in the photosynthetic processes of plants and bacteria. Work is currently underway to ascertain how porphyrins function, on a molecular level, in these biological systems. We are particularly interested in the relationship between the electronic properties of metalloporphyrins and their ability to bind ligands and participate in electron-transfer reactions. In this regard, we thought fast kinetic and spectroscopic investigations of nickel porphyrins might be very helpful in understanding such behavior. Nickel porphyrins are known to form complexes with basic ligands, such as piperidine, in the ground state [2–6]. Both the metal and the porphyrin ring can be oxidized [7]. Furthermore, more than one type of porphyrin cation radical ($a_{1u}$ versus $a_{2u}$) can be produced depending on the external substituents [8,9]. In order to make use of these potentially important properties in model system studies, it is first essential to understand the basic photophysics of these molecules. A consistent view of excited-state relaxation in nickel porphyrins has not been obtained from previous studies [10–12]. Therefore, we decided a thorough, systematic examination of nickel porphyrin photophysics and photochemistry was in order. In this paper we report on the first of such investigations from our laboratory.

Nickel porphyrins are non-luminescent. Neither fluorescence nor phosphorescence from the normal porphyrin manifold of excited states is observed [13]. Radiationless decay occurs rapidly to low-lying excited (dd) levels centered on nickel [1,8,10–12]. Thus, the photophysics of nickel porphyrins is dominated by the presence of these metal states. As we shall see, at least some of the photochemistry of these molecules is governed by the (dd) states as well. To understand this behavior fully, we must first examine the porphyrin and nickel electronic configurations and how they mix to form the new nickel porphyrin manifold of states.

0301-0104/83/0000–0000/$ 03.00 

### 1.1. Porphyrin states

Porphyrin electronic states and spectra can be explained on the basis of the four-orbital model [14–16]. Transitions occur from the two highest-filled molecular orbitals $a_{1u}(\pi)$ and $a_{2u}(\pi)$ to the lowest empty orbitals $e_g(\pi^*)$ Under $D_{4h}$ symmetry the latter are rigorously degenerate, while the former are accidentally so. The ground-state configuration $(a_{1u})^2\ (a_{2u})^2$ is, of course, a singlet state, $^1A_{1g}$. The excited configurations $(a_{1u}e_g)$ and $(a_{2u}e_g)$ are either singlet or triplet, depending on the relative spins of the promoted electron and the one remaining in the orbital with the hole

The success of the four-orbital approach in explaining porphyrin ground-state absorption spectra is due to the incorporation of strong configuration interaction between the singlets, $^1\psi_1 = {}^1(a_{1u}e_g)$ and $^1\psi_2 = {}^1(a_{2u}e_g)$ As shown previously [14], the symmetrical combination $^1B = 2^{-1/2}(^1\psi_1 + {}^1\psi_2)$ gives rise to the intense, near-UV Soret band, while the antisymmetric combination gives rise to the weaker, visible $^1Q$ bands.

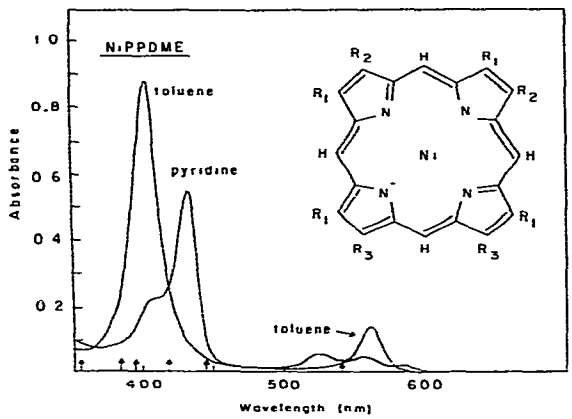


Fig 1 Ground-state absorption spectra for nickel protoporphyrin IX dimethylester (NiPPDME) in toluene and pyridine Sample concentrations are not the same in the two solvents Previous work [2,3] indicates that the extinction coefficient at the Soret band peak should be similar in toluene (four-coordinate nickel) and in pyridine (six-coordinate nickel). The arrows along the abscissa mark excitation wavelengths used in this study. They are from higher to lower energy, 355, 384, 395, 418, 445, and 532 nm. The inset shows structures for several "alkyl" substituted nickel porphyrins: octaethylporphyrin (OEP), $R_1 = R_2 = R_3 = R_4 =$ ethyl; PPDME, $R_1 =$ methyl, $R_2 =$ vinyl, $R_3 = CH_2CH_2COCH_3$; mesoporphyrin IX dimethyl ester, same as PPDME, but with $R_2 =$ ethyl, deuteroporphyrin IX dimethylester, same as PPDME, but with $R_2 = H$

In metalloporphyrins, which effectively possess $D_{4h}$ symmetry, there are generally two prominent visible bands, $^1Q(1,0)$ and $^1Q(0,0)$, the former being the first vibrational band (fig 1). The ratio of intensities of these two bands is determined primarily by vibronic coupling with the intense Soret band and is strongly influenced by the substituents on the porphyrin macrocycle [14,17,18]. For symmetry reasons, the triplets $^3\psi_1 = {}^3(a_{1u}e_g)$ and $^3\psi_2 = {}^3(a_{2u}e_g)$ do not interact in the first order, and remain essentially pure configurations [1,14–17].

### 1.2 Nickel states

Nickel (II) has a $d^8$ electronic configuration. When incorporated in a porphyrin, the nickel $d_{xy}$, $d_{xz}$ and $d_{yz}$ orbitals all contain two electrons no matter what the state of complexation of the metal to external ligands The $d_{xy}$ orbital is lowest in energy since its lobes point between the four porphyrin nitrogens in the plane of the macrocycle. In non-complexing solvents such as toluene, the nickel is in an essentially square-planar environment and the remaining two electrons go into the $d_{z^2}$ orbital. This is the ground-state configuration for four-coordinate nickel and is often designated $(d_{z^2})^2$ or in group-theoretical notation, $^1A_{1g}$. The lowest excited metal states are produced when one electron is promoted from the $d_{z^2}$ to the $d_{x^2-y^2}$ orbital. The latter is the highest in energy because of the nonbonding interaction, as its four lobes point toward the four nitrogens in the plane of the porphyrin ring The configuration $(d_{z^2}\, d_{x^2-y^2})$ gives rise to a singlet state, $^1B_{1g}$, and a triplet state, $^3B_{1g}$, depending on the relative directions of the two spins. By Hund's rule, the triplet is lower in energy.

### 1.3. Nickel porphyrin states

The theory for the states of nickel porphyrin complexes has been worked out previously [19]. Table 1 lists the new states produced by mixing the porphyrin and the nickel states discussed above. Transitions between states vertically displaced in table 1 involve mainly the porphyrin, while horizontal ones are basically transitions centered on nickel. Of course, some of the transitions are spin allowed, while others are not The new Q and B states arise from configuration interaction among the pertinent nickel porphyrin configura-

Table 1
Nickel porphyrin states from mixing [a]

| Porphyrin | Metal | | |
|---|---|---|---|
| | $^1A_{1g}$ | $^3B_{1g}$ | $^1B_{1g}$ |
| $^1\psi_0$ | $^1A_{1g}$ | $^3B_{1g}$ | $^1B_{1g}$ |
| $^3\psi_1$, $^3\psi_2$ | $^3T_1$, $^3T_2$ | $^{1,3,5}T_1$ $^{1,3,5}T_2$ | $^3T_1''$ $^3T_2''$ |
| $^1\psi_1$, $^1\psi_2$ | $^1Q$ $^1B$ | $^3Q_1$, $^3B$ | $^1Q$ , $^1B$ |

a) $^1\psi_1$ and $^1\psi_2$ have strong configuration interaction, whereas the $^3\psi_1$ and $^3\psi_2$ do not [19]

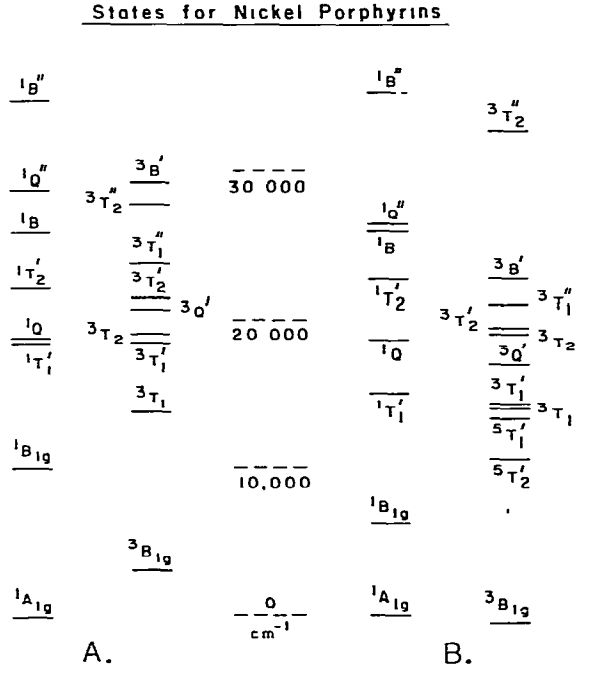


Fig 2 States and energies relative to $^1A_{1g}$ for nickel porphyrins from the calculations of Ake and Gouterman [19] The energy level spacings are shown for specific values of the $^3B_{1g}-^1A_{1g}$ energy gap (ETM) (A) Four-coordinate nickel (in-plane) with no external ligands and ETM = 3000 cm$^{-1}$. (B) Five-coordinate nickel (out-of-plane) with one external basic ligand and ETM = $-500$ cm$^{-1}$ The sample conditions used in the studies reported here favor six-coordinate nickel (in-plane) when complexation occurs, the energy level spacings are probably on the same order as those shown in B ($-1000$ cm$^{-1}$ < LTM < 0).

tions analogously to the porphyrin case, as discussed above, For example,

$$^3B' = 2^{-1/2}(^1\psi_1 \cdot {}^3B_{1g} + {}^1\psi_2 \cdot {}^3B_{1g}).$$

The lowest states that are most important for our discussion are those in the first row of table 1, they are formed by combining the nickel $^1A_{1g}$, $^1B_{1g}$, and $^3B_{1g}$ with the porphyrin $^1A_{1g}$ ground state. In non-complexing solvents, $^1A_{1g}$ is the ground state of the system and the molecule is diamagnetic. The energies of the other states relative to $^1A_{1g}$ for this four-coordinate, square-planar nickel in the porphyrin host are shown in fig. 2A [19]. This calculation is based on a $^3B_{1g}-^1A_{1g}$ energy gap (ETM) of 3000 cm$^{-1}$

### *1 4 Complexes with basic ligands*

The state energies are much different when the nickel becomes five-coordinate by picking up one ligand such as pyridine (fig. 2B). As we shall discuss, our experiments are carried out under conditions where the contributions from five-coordinate nickel are minimized, but rather six-coordination predominates in the basic solvents used However, the differences observed between figs. 2A and 2B illustrate the effect of coordination on the nickel porphyrin states and fig. 2B gives relative energies approximating those expected for six-coordination

In five-coordination the nickel moves out of plane. The filled $d_{z^2}$ orbital is destabilized by interaction with the nitrogen p orbital on the base and moves closer in energy to the empty $d_{x^2-y^2}$ orbital The further out of plane the nickel moves, the lower in energy the states involving excited nickel configurations become, as compared to $^1A_{1g}$. Fig. 2B illustrates the case where nickel has moved far enough out of plane, and the $d_{z^2}$ orbital has been destabilized enough, so that $^3B_{1g}$ has become the ground state. The molecule is paramagnetic A porphyrin-type visible spectrum is still predicted, but it will be red-shifted.

$^1B_{1g}$, $^3B_{1g}$ and many of the higher states will also be lowered in energy relative to $^1A_{1g}$ if the porphyrin picks up two ligands This produces six-coordinate nickel in an octahedral environment, the nickel atom is in the plane of the porphyrin ring Analogous inorganic complexes of nickel are essentially always paramagnetic, reflective of a $^3B_{1g}$ ground state, as the $d_{z^2}$ orbital is destabilized to a point that the energy for

promoting an electron to the $d_{x^2-y^2}$ orbital is less than the pairing energy [20]. From the point of view of general inorganic chemistry, five-coordination is rather unusual for Ni(II) [21]. Thus, for strongly basic ligands and/or porphyrin macrocycles that make nickel acidic enough, one expects $^3B_{1g}$ to be lower in energy than $^1A_{1g}$ by up to several thousand wavenumbers for the six-coordinate complex. Six-coordination will also stabilize $^1B_{1g}$ and bring it down closer in energy to $^1A_{1g}$.

This view is consistent with the behavior observed for a variety of nickel porphyrins in the presence of basic ligands such as pyridine, piperidine, *n*-butylamine, etc. The state of complexation, equilibrium constants for complex formation, and the question of paramagnetic versus diamagnetic ground states in nickel porphyrins have been investigated extensively by spectrophotometric titration, NMR chemical shifts and line broadening, and magnetic susceptibility [2–6,22]. To summarize, it was concluded from studies with chloroform/pyridine or chloroform/piperidine and other solvent mixtures with substituted mesoporphyrin or deuteroporphyrin IX dimethylester (see fig. 1 insert and caption for the porphyrin structures) that an increase in solvent basicity, a decrease in temperature, or a decrease in porphyrin basicity (increase in electron-withdrawing groups on the porphyrin periphery) favors the reversible formation of six-coordinate octahedral species over the four-coordinate square-planar one [2,3] Evidence for five-coordinate complexes is generally found only at low concentration of basic ligands [2,3, 6,22]. Evidence for a contribution from five-coordinate species has also been reported for porphyrins with very strong electron-withdrawing groups, such as $NO_2$ [3] Again, this appears to occur only at low ligand concentrations. Here, we have studied nickel octaethylporphyrin (NiOEP) and nickel protoporphyrin IX dimethylester (NiPPDME), and have employed neat solvents of moderate (pyridine, $pK_b$ = 8 64) or strong (piperidine, $pK_b$ = 2.80) basicity. Under these conditions, the contribution from five-coordinate species appears to be minimal. Toluene is used as the solvent for studies of four-coordinate (*un*complexed) nickel porphyrin photophysics.

### *1.5. Previous studies*

Investigations of nickel porphyrin luminescence have shown that these molecules are "dark"; no emission verifiable by excitation spectra has been found [13] It has been concluded that the normally emissive porphyrin levels $^1Q$, $^3T_1$ and $^3T_2$ are quenched rapidly by the low-lying $^1B_{1g}$ and/or $^3B_{1g}$ (dd) states. Previous attempts using picosecond techniques to elucidate the decay pathways and kinetics have produced contradictory conclusions [10–12]. Kobayashi et al [10] investigated NiPPDME in benzene and reported kinetics at two wavelengths, but presented no transient spectra Decay of the transient absorbance at 480 nm gave two components with lifetimes of 12 ± 2 ps and 250 ± 50 ps Recovery of the ground-state bleaching at 560 nm showed only the 250 ps step. The authors considered several possible decay pathways, including the following (see fig 2A):

$$^1Q \rightarrow {}^1B_{1g} \ (\approx 10 \text{ ps}), \qquad (1i)$$

$$^1B_{1g} \rightarrow {}^1A_{1g} \ (\approx 250 \text{ ps}); \qquad (1ii)$$

$$^1Q \rightarrow {}^3T_1 \ (< 10 \text{ ps}), \qquad (2i)$$

$$^3T_1 \rightarrow {}^3B_{1g} \ (\approx 10 \text{ ps}), \qquad (2ii)$$

$$^3B_{1g} \rightarrow {}^1A_{1g} \ (\approx 250 \text{ ps}), \qquad (2iii)$$

$$^1Q \rightarrow {}^1B_{1g} \ (< 10 \text{ ps}), \qquad (3i)$$

$$^1B_{1g} \rightarrow {}^3B_{1g} \ (\approx 10 \text{ ps}), \qquad (3ii)$$

$$^3B_{1g} \rightarrow {}^1A_{1g} \ (\approx 250 \text{ ps}). \qquad (3iii)$$

Kobayashi et al. [10] favored the pathways (1i) and (1ii), which we term route (1) They ruled out routes (2) and (3) because these require intersystem crossings, all of which the authors thought too slow to account for the observed behavior. This view was based on an energy gap law developed for intersystem crossing between ($\pi\pi^*$) states of large aromatic molecules [23]. However, this law may not be rigorously applicable here and intersystem crossing might be expected to be much faster (see below).

Chirvonyi et al. [11] showed a transient spectrum at one delay time for NiOEP in toluene. They observed a single component having a 270 ± 50 ps time constant, and favored route (2) on the basis of the red-shifted, porphyrin-type transient spectrum. In a second paper

Chirvonyi et al. [12] drew similar conclusions from a study of Ni-deuteroporphyrin IX dimethyl ester in toluene. A 10 ps step was attributed to decay of $^3T_1$ [path (2ii)]. They investigated the same porphyrin in piperidine (six-coordinate, paramagnetic ground state) and reported spectra at "0" ps and 50 ps after excitation at 532 nm. On the basis of the 50 ps spectrum, it was concluded that the ligands had fallen off in the excited state, and that ≈100 ns is required for them to come back on. The "0" ps spectrum was assigned to $^3T_1$. Our results unambiguously demonstrate that ligands can fall off in similar porphyrins in both pyridine and piperidine, following excitation at the appropriate wavelengths, but we differ with Chirvonyi et al. [12] on the assignment of the states involved. Furthermore, we show that the results of excitation at more than one wavelength in complexing solvents must be compared, since either complexed or uncomplexed species present in the ground-state equilibrium mixture can be pumped depending on the excitation wavelength. The net result of photon absorption can be ligand binding, ligand release, or complete relaxation to the ground state in several hundred picoseconds. In this paper we report the results of our studies on the excited-state dynamics of several nickel porphyrins.

## 2. Experimental

The picosecond apparatus is based on a Quantel YG400 laser system that delivers single, 33 ps, 1064 nm, 10 mJ pulses at a 10 Hz repetition rate. Radiation at 1064 nm is split equally into two parts with a beam splitter to drive the excitation and monitoring (pump and probe) legs of the apparatus. In the excitation leg, radiation at 1064 nm can be converted to the harmonics at 532, 355, and 266 nm in KD*P crystals. For a particular configuration of crystals, the unwanted residual radiation is removed from the desired harmonic with dichroic and colored glass filters. Any of the harmonics can be used directly to excite the sample by focusing to a 1.5–2 mm diameter spot in a 2 mm pathlength sample cuvette, or can be sent first through an additional wavelength-shifting device. The 532 and 355 nm light can be used to generate pulses at longer wavelengths by stimulated Raman scattering in suitable liquids. Pulses at the Stokes–Raman harmonic wavelengths of 395 and 445 nm are obtained by focusing the 355 nm pulses into a 5 cm cell of cyclohexane. Similarly, flashes at 384 and 418 nm are produced when perdeuterocyclohexane is used as the Raman liquid. Extreme care was taken to avoid non-linear effects in the sample by keeping the excitation intensities low and building up signals by signal averaging. The 532 nm pulses were reduced to 300 μJ of energy, while those in the violet and blue were less than 100 μJ per pulse.

The 1064 nm radiation in the probe leg of the apparatus traverses a stepping-motor driven optical delay line. Delays from minus several hundred ps to ≈12 ns can be obtained. The broad-band monitoring pulses are generated by focusing the 1064 nm pulses into a cell containing $CCl_4/CHCl_3$ = 6/4. We find that this mixture gives the most spectrally "flat" continuum over the 500–900 nm region of any liquid we have tried. This is essential for 2D detection. The probe pulses are also of ≈30 ps duration and extend from 450 nm through the visible and past 1064 nm into the IR. The 1064 nm light is removed with a dichroic beam splitter. The "white" probe light is passed through a pair of cylindrical lenses and is focused at the sample as a 1 mm wide by 2 cm high vertical slit. The white light then passes through two pinholes placed immediately behind the sample. (The pump light passes through only one of the pinholes, defining the excited region of the sample.) The probe light subsequently passes through colored glass and neutral density filters and is focused onto the entrance slit of a 1/4 m Jarrell–Ash monochromator containing a 13.2 nm/mm dispersion grating. A PAR 1205B vidicon detector is placed at the output of the monochromator and is coupled to the 1205A optical multichannel analyzer (OMA) console, fitted with a 2D option card. The two 500-channel vidicon tracks are set so that one is aligned with the dispersed spectrum of probe light passing through the excited sample, while the second is aligned with the light transmitted through the unexcited or reference region of the sample. The digitized spectral information is transferred from the two OMA memories to a Cromemco Z-80 microcomputer. Operation of a 1205 OMA in the 2D-mode and interfacing procedures are described elsewhere [24,25]. Baseline and dark current subtraction, calculation of the absorption changes, signal averaging, display, and data storage are all handled by the computer, which also controls shutters in the pump and probe legs and the stepping motor driving the delay line.

Spectra of neutral density filters are routinely checked on the picosecond system by blocking the pump beam and placing a filter in front of the "excited" region of the sample during the appropriate data acquisition cycle. This precautionary procedure is essential to ensure that invalid peaks and troughs in the transient spectrum are not introduced because of the dynamic range of the vidicon in spectral regions where very high or very low probe light intensities are transmitted through the sample.

A completely corrected transient absorption spectrum over a 170 nm interval comprising the average of ≈300 laser excitation pulses takes ≈10 min to acquire, plot and store on floppy disk. Standard deviations in $\Delta A$ over the wavelength regions shown in this paper are typically ±0.005.

All data were taken at room temperature with an all teflon and glass flow system operated at a rate sufficient to provide fresh sample in the excited region for each laser pulse. However, it was found that little, if any, decomposition of the samples occurred after several thousand laser shots even if they were not flowed. Low excitation intensities are helpful in this regard. Sample concentrations were adjusted to give a maximum absorbance in the Q-band region (500–600 nm) between 0 3 and 0 5 in a 2 mm pathlength cell. Spectral grade solvents were used. Nickel porphyrins were purchased from Porphyrin Products (Logan, Utah) and their purity checked by TLC and absorption spectroscopy. No emission was observed from any of the samples.

Table 2
Ground-state absorption spectra of nickel porphyrins [a]

| Compound | Solvent | B(0,0) | Q(1,0) | Q(0,0) |
|---|---|---|---|---|
| NiOEP | toluene | 393 (10 8) | 516 (0 35) | 552 (1.0) |
| | pyridine | 393 (9 74) | 516 (0.30) | 552 (1.0) |
| | piperidine | 419 (9.39) | | 552 (1.7) |
| | | 393 (41.3) | 542 (1 83) | 574 (1 0) |
| NiPPDME | toluene | 403 (4.89) | 525 (2.89) | 562 (1.0) |
| | pyridine | 403 (11.0) | 525 (0 3) | b) |
| | | 433 (27 5) | b) | 585 (1 0) |
| | piperidine | 403 (3.68) | | |
| | | 431 (23.9) | 552 (1.57) | 585 (1 0) |
| NiMeso | toluene | 393 (5 87) | 516 (0 31) | 552 (1.0) |
| | pyridine | 393 (6 02) | 516 (0 34) | 552 (1 0) |
| | | 420 (1.86) | | |
| | piperidine | 420 (6 50) | | 552 (1 25) |
| | | 393 (46.9) | 542 (1 75) | 574 (1.0) |

a) Peak wavelength in nm; numbers in parentheses are peak heights relative to Q(0,0). Note that in certain solvents there are two peaks of each type, due to the presence of both four- and six-coordinate species See figs. 3C and 4C.

b) A peak at 555 nm (relative height of 2 25) is resolvable, but represents a mixture of the uncomplexed Q(0,0) band at 562 nm (see toluene data) and the complexed Q(1,0) band at 552 nm (see piperidine data)

### 3. Results and discussion

Typical absorption spectra and nickel porphyrin structures are shown in fig 1. We discuss in detail the results for nickel octaethylporphyrin (NiOEP) and nickel protoporphyrin IX dimethylester (NiPPDME). Peak wavelengths and relative intensities for the ground-state absorption spectra in toluene, pyridine and piperidine are summarized in table 2. In some solvents, both four-coodinate and six-coordinate species are present in the ground state, and for these cases two bands of a particular type can be resolved. The relative contribution of four- and six-coordinate species will be discussed along with the data for each system.

We have observed a variety of photophysical and photochemical behavior for the nickel porphyrins in the three solvents employed. There appear to be several general "rules" that, to a large extent, govern this behavior.

(1) Intersystem crossing in the upper manifold is rapid. Relaxation to the lowest "excited" state is fast (generally ≤ 15 ps), no matter what its multiplicity or that of the ground state.

(2) The nickel $^1A_{1g}$ state with two (extra) ligands attached is unfavorable. In a basic solvent, if a decay route proceeds through a state containing substantial nickel $^1A_{1g}$ character, such as $^1A_{1g}(L)_2$ or $^1Q(L)_2$, the ligands will probably fall off.

(3) The nickel $^1B_{1g}$ and $^3B_{1g}$ states have an affinity for basic ligands. In a basic solvent, if a decay route proceeds through either of these levels, then generally two ligands will be picked up to give $^1B_{1g}(L)_2$ or $^3B_{1g}(L)_2$. A similar fate exists for states containing an admixture of either the nickel $^1B_{1g}$ or $^3B_{1g}$ configurations.

Rules (2) and (3) follow from the effect of basic ligands on the nickel $d_{x^2-y^2}$ versus $d_{z^2}$ energy gap, as

discussed in section 1. The rules are consistent with the experimental data of other workers

Although we have presented the data for the two porphyrins in the three solvents as individual subsections, it is essential to compare the results under the various conditions to fully understand the behavior in any one of them

### 3.1 NiOEP and NiPPDME in toluene

Both porphyrins exhibit essentially identical photophysical behavior, independent of the excitation wavelength employed (355, 384, 395, 418, 445, and 532 nm). The transient spectra, examples shown in figs 3A, 4A and 5, exhibit bleaching in the Q-bands appearing

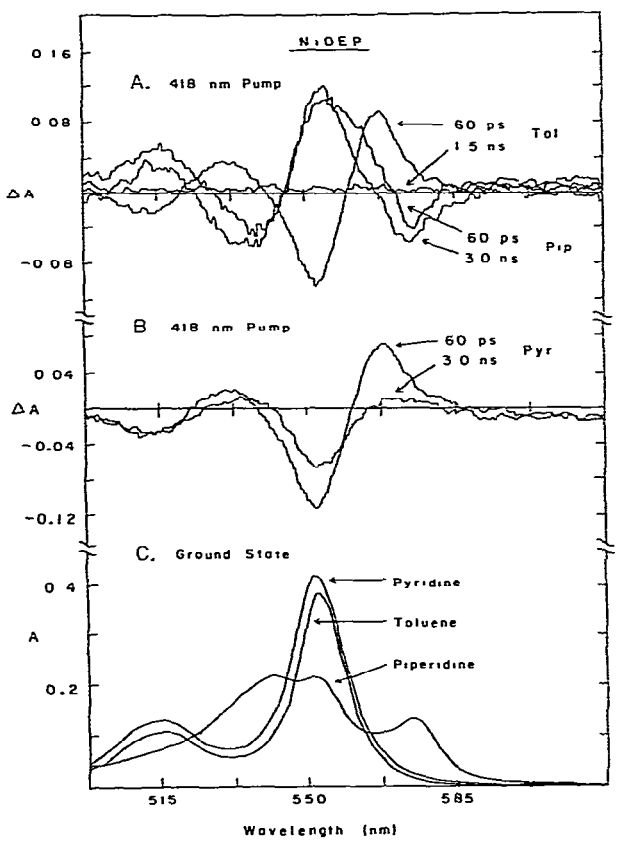


Fig 3 The top two panels show Q-band region transient absorption spectra for NiOEP in toluene and piperidine (A) and in pyridine (B) following excitation at 418 nm Ground-state absorption spectra in the same region (C).

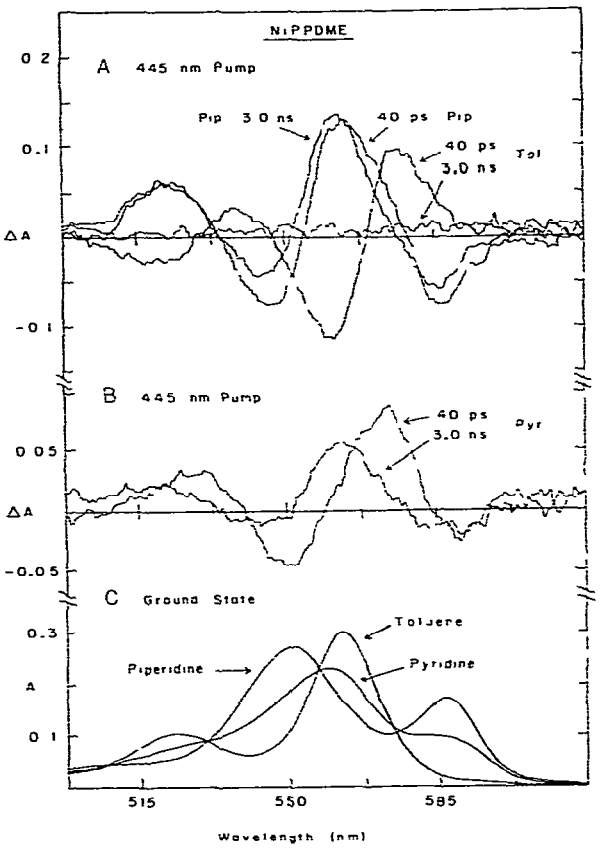


Fig 4. Spectra for NiOEP. Difference spectra in toluene and piperidine (A) and in pyridine (B) following excitation at 445 nm Ground-state Q-bands (C).

with the pulse-limited risetime (figs. 5A, and triangles in figs 6A and 6B). Two new strong absorption peaks with maxima red-shifted from the ground-state bands by 15 nm NiOEP and by 20 nm in NiPPDME are well resolved This transient absorption spectrum appears to lag development of the ground-state bleaching by 10–15 ps (compare circles and triangles in figs. 6A and 6B). Close examination of fig. 5A shows that part of this lag is due to the evolution of a shoulder on the red side of this band Analysis of this kinetic behavior indicates that the short-lived feature decays with a time constant of 10–15 ps The shoulder and the lag are seen for both NiOEP and NiPPDME in toluene. The decay of the strong transient absorptions and recovery of the ground-state bleachings give single exponentials with an average time constant of 280 ± 20 ps

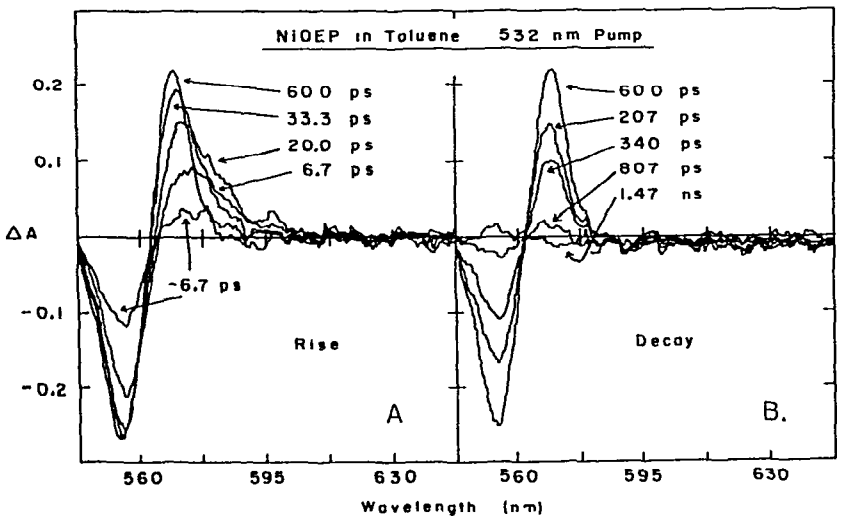


Fig. 5. Difference spectra as a function of time for NiOEP in toluene after excitation with 532 nm flashes. The spectra have $\Delta A = 0$ to the longest wavelength monitored, 715 nm. The rapid growth and decay of the shoulder on the red side of the strong transient absorption peak can be seen in (A). NiPPDME gives similar behavior in toluene (not shown). Kinetic plots are shown in fig. 6.

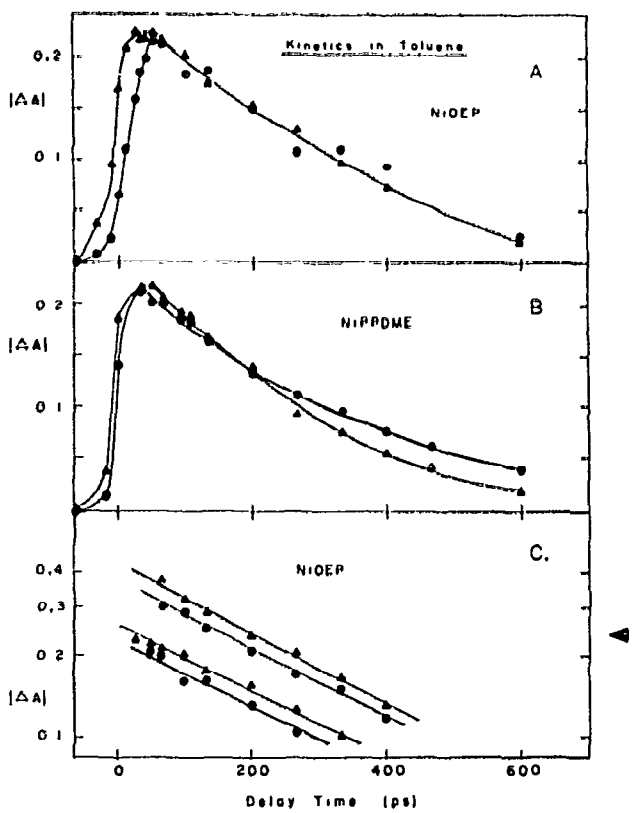


(figs. 5B and 6). These spectral and kinetic data agree, where comparisons can be made, with the observations of Kobayashi et al. [10] and Chirvonyi et al. [11]. However, there are differences in the interpretation of the data.

The transient behavior just described appears to be representative of the photophysics of nickel porphyrins in non-complexing solvents. The nickel is four-coordinate and the ground-state for both porphyrins is $^1A_{1g}$. The lowest excited state is $^3B_{1g}$, produced by combining the porphyrin $^1A_{1g}$ ground and the nickel excited $^3B_{1g}$, $^3(d_{z^2}\, d_{x^2-y^2})$, configurations. This situation

Fig. 6. Kinetics in toluene of the bleaching in the Q(0,0) band (○) for NiOEP at 553 nm (A) and NiPPDME at 559 nm (B), and the strong long-wavelength transient absorption band (●) for NiOEP at 567 nm (A) and NiPPDME at 578 nm (B). Panel (A) for NiOEP with 532 nm flashes is for the data of fig. 5. The upper two traces of panel (C) show the same data plotted on a log scale. The lower two traces of (C) are for NiOEP with the same two monitoring wavelengths, but with 355 nm flashes. Panel (B) shows data for NiPPDME produced by excitation at 532 nm. The results of at least three sets of measurements for each porphyrin gives a time constant of 280 ± 20 ps. Absorption changes in (A) and (C) are normalized to the maximum value for the bleaching in order to more clearly show the lag in the formation of the transient absorption band (see text).

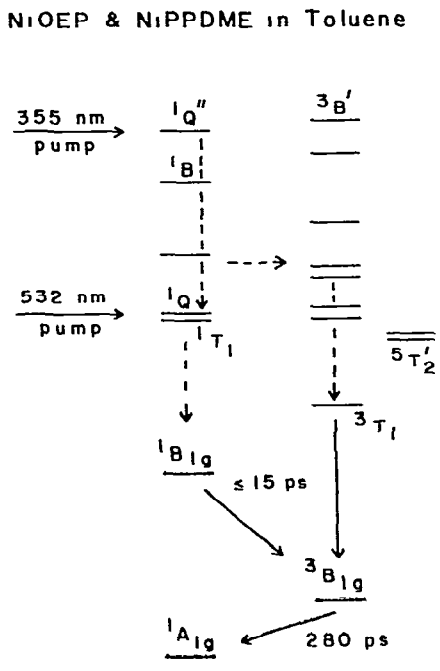


Fig 7 State diagram summarizing the interpretation of the data for the photophysical behavior of nickel porphyrins in toluene. (In this figure and in figs 10 and 12, dashed arrows are shown where more than one decay path is likely while solid arrows indicate the probable dominance of one relaxation route Dotted arrows show possible, less likely routes.) The states reached by 532 or 355 nm flashes are indicated by horizontal arrows. This figure is based on an E1M of 3000 $cm^{-1}$, the same as fig. 2A.

is presented diagramatically in fig 7 along with the relaxation pathways most consistent with all the observations

Excitation into the excited singlet-state manifold is followed by rapid intersystem crossing and relaxation to $^3T_1$. Some relaxation in the upper singlet manifold to $^1Q$ or $^1T_1'$ (whichever is lower) also occurs. Relaxations $^3T_1 \rightarrow {}^3B_{1g}$ and $^1Q$ (or $^1T_1'$) $\rightarrow {}^1B_{1g}$ take $\leq 10$ ps. In spectra taken at short delays following excitation (fig 5A), the Q(0,0) band of $^1B_{1g}$ appears as a shoulder on the red side of the strong transient absorption band, which we assign as the Q(0,0) transition of $^3B_{1g}$. Intersystem crossing $^1B_{1g} \rightarrow {}^3B_{1g}$ requires 10–15 ps. Thus, the 10–15 ps lag observed for the long-wavelength band to reach its maximum is due to all these relaxation processes Decay of the lowest excited state, $^3B_{1g} \rightarrow {}^1A_{1g}$, is then responsible for the 280 ± 20 ps step (figs. 5B and 6) Thus, rule (1) dominates the behavior.

This interpretation of the results is a combination of routes (2) and (3) discussed in section 1. Route (2) is the relaxation pathway preferred by Chirvonyi et al [11,12] Route (1) is the one favored by Kobayashi et al. [10] in which $^1B_{1g}$ is responsible for the 250–300 ps step Route (3) is deemed unlikely by both of these groups The relaxation routes involving $^3B_{1g}$ (fig 7) give the most reasonable explanation of all of our results for the nickel porphyrins in the three solvents studied, and is also consistent with data for other transition-metal porphyrin and inorganic complexes Serpone et al [26] argue from their observations on osmium porphyrins that lowest triplet states are formed in high yield, no matter whether they are ($\pi\pi^*$) or (dd) in character, following excitation into the upper singlet manifold Rapid intersystem crossing into the triplet manifold has been suggested for iron porphyrins as well [27] It is generally found for inorganic transition-metal complexes that relaxation to the lowest excited state must be rapid (< 15 ps), since most of the observed emission and photochemical activity appears to occur from there [28] These data are consistent with the contention that the relaxation proceeds mainly through $^3B_{1g}$ in nickel porphyrins in non-complexing solvents We should examine all of the arguments used previously to support either $^3B_{1g}$ or $^1B_{1g}$ in more detail along with further discussion of the decay routes in fig 7.

Kobayashi et al. [10] studied NiPPDME in benzene and observed an ≈250 ps step for the recovery of the ground-state bleaching at 560 nm and for decay of the excited-state absorption at 480 nm They found an additional 12 ps component at 480 nm only Spectral data were not presented They deduced that the Franck–Condon factors would be too small and, thus, the rate of intersystem crossing, $^3B_{1g} \rightarrow {}^1A_{1g}$, too slow to account for the 250 ps kinetics, even in view of the estimated small 3000 $cm^{-1}$ energy gap from the calculations of Ake and Gouterman [19] On similar grounds, they excluded the possible importance of the $^1B_{1g}$ to $^3B_{1g}$ conversion Thus, routes (2) and (3) were ruled out These conclusions were based on the energy gap law developed for intersystem crossing between ($\pi\pi^*$) states of large aromatic molecules [23]. However, this law may not be rigorously applicable here and intersystem crossing might be expected to be much faster for

a number of reasons. (1) the transitions just considered are between states with significant (dd) character, (2) there is substantial mixing between the porphyrin and nickel configurations (singlet and triplet) as discussed above (table 1), and, (3) there are a number of additional states resulting from this mixing that provide an increased density of states that would facilitate intersystem crossing and rapid relaxation in the upper manifold. On the basis of points (1) and (2) and the previous discussion, we suggest that a time constant of several hundred picoseconds is not unreasonable for the conversion $^3B_{1g} \rightarrow {}^1A_{1g}$ On the basis of points (2) and (3), we suggest that intersystem crossing to and fast relaxation in the upper triplet manifold should be rapid (< 10 ps)

Chirvonyi et al. [11] preferred $^3B_{1g}$ [route (2)] on the basis of the red-shifted transient spectrum, which is similar to the normal porphyrin ground-state spectrum. The observation is clearly seen by comparing the transient absorption peaks 60 ps after excitation in toluene (figs 3A and 4A) with the ground-state spectra in piperidine (figs. 3C and 4C). However, a close examination of table 1, fig 2A, and the calculations of Ake and Gouterman [19] indicates that $^1B_{1g}$ should have a spectrum similar to that of $^3B_{1g}$ The electronic transition that gives rise to the transient absorption in the visible region for *both* $^1B_{1g}$ and $^3B_{1g}$ derives most of its oscillator strength from the normal porphyrin Q-band transition, $^1\psi_0 \rightarrow {}^1Q = 2^{-1/2}(^1\psi_1 - {}^1\psi_2)$, but with the upper states containing an admixture of the porphyrin $^1\psi_1$ and $^1\psi_2$ with either the nickel $^1B_{1g}$ or $^3B_{1g}$, respectively (table 1). Therefore, the transient spectra observed by Chirvonyi et al [11,12] or by ourselves (figs. 3A, 4A, and 5) 40 ps and longer after excitation for the nickel porphyrins in toluene cannot be assigned to $^3B_{1g}$ over $^1B_{1g}$ simply on the basis of a red shifted, double-banded visible spectrum.

Chirvonyi et al. [12] also observed a spectrum "0" ps after excitation for deuteroporphyrin IX dimethylester in toluene and attributed it to T–T absorption. A more reasonable view is the spectrum is comprised of contributions from $^3T_1$, $^1B_{1g}$, and $^3B_{1g}$, with the $^3T_1$ and $^1B_{1g}$ components disappearing with a time constant of 10–15 ps. The conversion $^1B_{1g} \rightarrow {}^3B_{1g}$ should be faster than the time of 280 ps that we and Chirvonyi et al. [11,12] attribute to the $^3B_{1g} \rightarrow {}^1A_{1g}$ step. The former involves a spin flip of one electron in the $(d_{z^2}\, d_{x^2-y^2})$ configuration, while the latter requires a spin flip as well as a change from $(d_{z^2}\, d_{x^2-y^2})$ to $(d_{z^2})^2$ Whether or not the $^1B_{1g} \rightarrow {}^3B_{1g}$ time constant is as fast as 10 ps is difficult to state a priori, but seems reasonable. We have stated that one expects $^1B_{1g}$ to absorb in the same regions of the spectrum as $^3B_{1g}$. On this basis the most reasonable explanation for the rapidly decaying (≈ 10–15 ps kinetics) shoulder on the red side of the strong band at 572 nm for NiOEP in toluene (fig. 5A) is due to $^1B_{1g}$. The "0" ps spectrum of Chironyi et al. [12] does indeed have an absorption tail extending ≈ 10 nm to the red of the long-wavelength band observed in their 50 ps spectrum This is consistent with our spectra for both NiOEP and NiPPDME in toluene and for NiOEP in pyridine discussed below.

The spectra of fig 5A for NiOEP and those for NiPPDME (not shown) indicate that there is also some prompt absorption at the same wavelength as the absorption maximum assigned to $^3B_{1g}$ This observation indicates that $^3B_{1g}$ is also populated partially from $^3T_1$. In addition, the finding by Kobayashi et al. [10] of a large 12 ps component to the transient absorption at 480 nm for NiOEP in benzene is suggestive of a $^3T_1$ or $^1Q$ contribution to spectra taken very early after the flash On the basis of all these data, the most likely explanation is that $^1B_{1g}$ absorbs 5–10 nm to the red of $^3B_{1g}$ and gives rise to most, if not all, of the shoulder on the Q(0,0) band of the $^3B_{1g}$ transient (fig. 5A). The Q(1,0) band of $^1B_{1g}$ is obscured by bleaching in the ground-state Q(0,0) band near 550 nm. The decay $^1B_{1g} \rightarrow {}^3B_{1g}$ gives rise to part of a 10–15 ps lag observed in the formation of $^3B_{1g}$ (fig. 6) $^3T_1$ (and $^1Q$) have little absorption in the 570–600 nm region and, therefore, give rise to the remainder of the lag Thus, it appears that $^3B_{1g}$ is fed by both $^3T_1$ [route (2)] and $^1B_{1g}$ [route (3)] as shown in fig. 7.

To summarize the data for NiOEP and NiPPDME in toluene, the relaxation pathways proceeding through $^3B_{1g}$, appear to dominant the radiationless deactivation [rule (1)]. This lowest excited state is reached by two pathways, internal conversion from $^3T_1$ and intersystem crossing from $^1B_{1g}$. The two routes give rise to a 10–15 ps lag in the formation of $^3B_{1g}$. The 280 ps decay is assigned to $^3B_{1g} \rightarrow {}^1A_{1g}$. As discussed in detail above this interpretation is consistent with (1) all of the picosecond spectral and kinetic data in toluene, particularly when consideration is made of the types of transitions involved, (2) the availability of

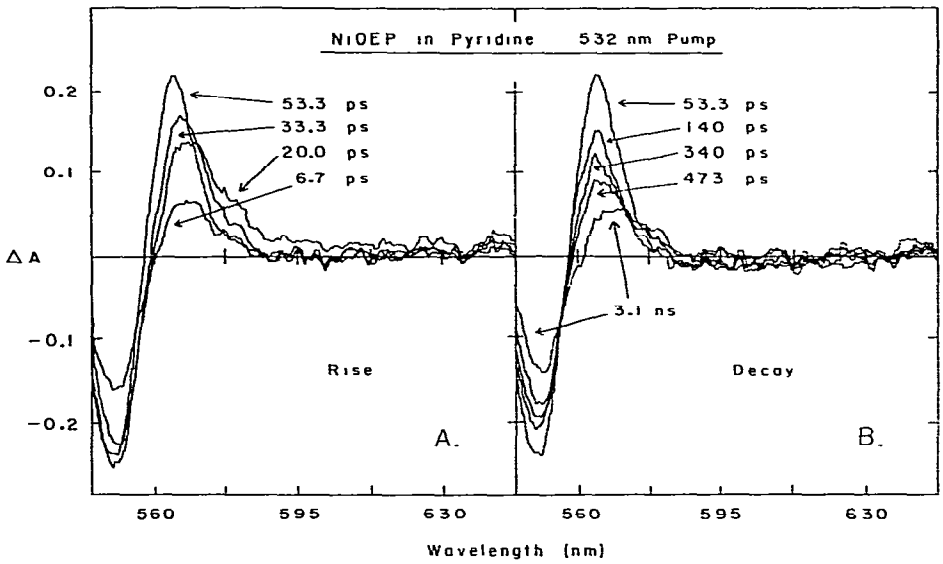


Fig. 8 Difference spectra as a function of time for NiOEP in pyridine produced by 532 nm flashes. The spectra show $\Delta A \approx 0$ to 715 nm, the longest wavelength monitored

efficient routes for intersystem crossing, especially in the upper manifold, (3) the photophysical and photochemical behavior observed for other transition metal porphyrins and many inorganic transition metal complexes, and (4) the data for NiOEP and NIPPDME in pyridine and piperidine to be discussed below

*3.2. NiOEP in pyridine*

The equilibrium constant for the formation of a six-coordinate complex between NiOEP and pyridine in the ground state is extremely low. The ground state remains $^1A_{1g}$. The absorption spectrum is essentially identical with that in toluene (table 2 and fig. 3C). The transient spectrum to delays of several hundred ps (figs. 3B and 8A) is also identical to that found in toluene (figs. 3A and 5A). On the basis of this comparison and the previous discussion, we assign this spectrum to $^3B_{1g}$. We attribute the initial shoulder on its long-wavelength absorption band to $^1B_{1g}$. This fast transient and the probable lack of absorbance due to $^3T_1$ in this region give rise to the clear lag of 10–20 ps in the appearance of the long-wavelength band as compared to the ground-state bleaching (figs. 8A and 9A). The decay of 450 ± 35 ps (figs. 8B and 9A), which is thus assigned to $^3B_{1g}$, is slower than in toluene. We return to this point below.

The 450 ps decay appears to occur by two paths, as illustrated in fig. 10. Intersystem crossing to $^1A_{1g}$ gives a partial recovery of the ground-state bleaching (figs. 3B and 8B). The other pathway is a manifestation of rule (3), and $^3B_{1g}$ picks up two pyridines to produce the complex $^3B_{1g}(pyr)_2$. This results in the formation of a red-shifted transient difference spectrum, shown clearly in fig. 8B at 3.1 ns after 532 nm excitation. The absorption peaks of this transient are at nearly the same wavelengths as those found for the complexed $^3B_{1g}(pip)_2$ ground state of NiOEP in piperidine. This is evidenced by the bleaching in the transient spectra in piperidine of fig. 3A and the ground-state absorption spectrum in fig. 3C. (Below we discuss the $^3B_{1g}(pip)_2$ ground state in piperidine.) This new state decays with a time constant of 10–20 ns (fig. 9A), requiring conversion of $^3B_{1g}$ to $^1A_{1g}$ as well as loss of two ligands (fig. 10). The process is expected to be temperature dependent.

That the long-lived state for NiOEP in pyridine is $^3B_{1g}(pyr)_2$ provides further support to the assignment of the 450 ps state in pyridine as well as the 280 ps state in toluene, having the same absorption spectra.

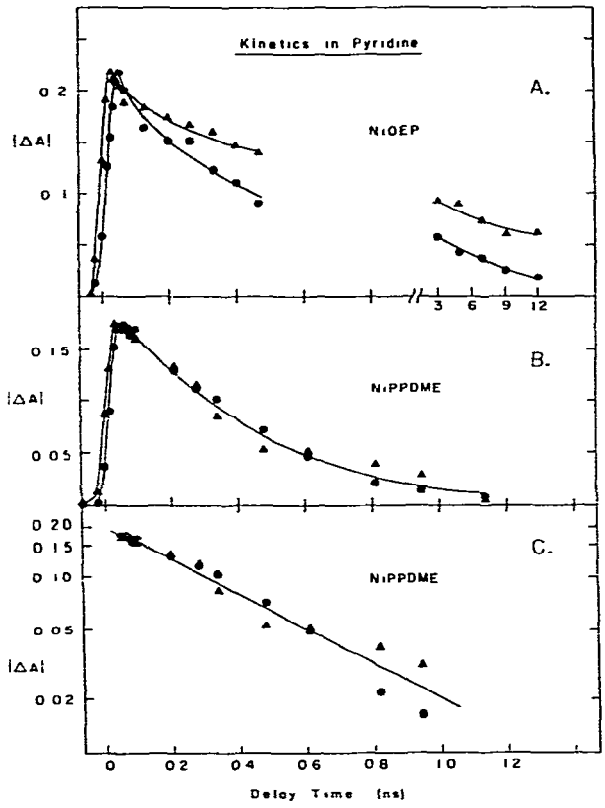


Fig 9 Kinetics in pyridine produced by 532 nm flashes of the bleaching (▲) for NiOEP at 553 nm (A) and NiPPDME at 553 nm (B and C) and of the strong long-wavelength transient absorption band (●) for NiOEP at 567 nm (A) and for NiPPDME at 572 nm (B and C) The plot for NiOEP is for the same data of fig 8, showing the long-lived component with a lifetime of 10–20 ns The initial component for NiOEP and the complete decay for NiPPDME in pyridine have a time constant of 450 ± 35 ps Three sets of measurements on each compound were carried out

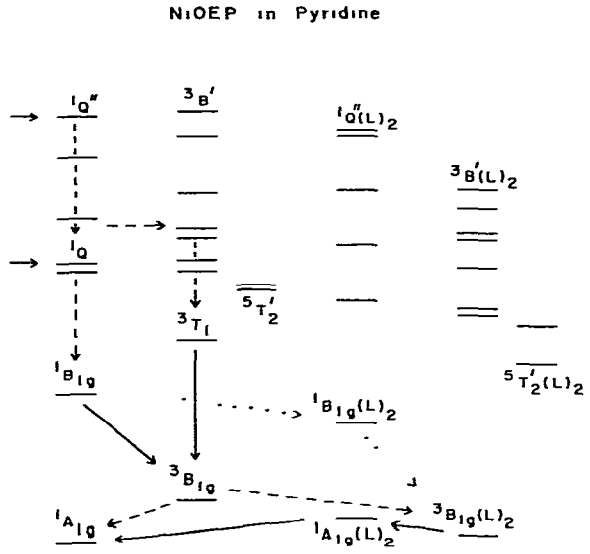


fig. 10. State diagram summarizing the photophysical and photochemical behavior for NiOEP in pyridine The molecule is uncomplexed in the $^1A_{1g}$ ground state but picks up two pyridines in $^3B_{1g}$. The decay of $^3B_{1g}$ by the two pathways shown is 450 ps Release of the ligands by the two $^3B_{1g}(pyr)_2$ takes 10–20 ns The energy of the latter state above the $^1A_{1g}$ is probably 1000 $cm^{-1}$ or more.

to $^3B_{1g}$. This analysis is also consistent with the assignment of the rapidly decaying shoulder on the long-wavelength $^3B_{1g}$ band to $^1B_{1g}$ The latter is probably the only state above $^3B_{1g}$ that has absorbance in the region. Most of the $^1B_{1g}$ state intersystem crosses to $^3B_{1g}$ with a $\leq$ 10–15 ps time constant. It is also possible that some $^1B_{1g}$ pick up two ligands [rule (3)] to give $^1B_{1g}(pyr)_2$, followed by rapid ($\leq$ 10 ps) intersystem crossing to $^3B_{1g}(pyr)_2$. However, we have no firm evidence that the latter process occurs (fig. 10).

The longer decay time assigned to $^3B_{1g}$ of 450 ps in pyridine versus 280 ps in toluene suggests that intersystem crossing $^3B_{1g} \rightarrow {}^1A_{1g}$ is slower in pyridine than in toluene The decay is also 450 ps for NiPPDME in pyridine and for both NiOEP and NiPPDME in piperidine. Thus, pyridine and piperidine exert a solvent effect that slows intersystem crossing $^3B_{1g} \rightarrow {}^1A_{1g}$. Examination of table 1 indicates that this process requires a spin flip and conversion of $(d_{z^2}\, d_{x^2-y^2})$ to $(d_{z^2})^2$ on nickel. One might expect that any effect that would change the energy gap between $d_{z^2}$ and $d_{x^2-y^2}$ could change the rate of the intersystem crossing The $^3T_1 \rightarrow {}^3B_{1g}$ step also requires this conversion. Comparison of figs. 5A and 8A indicates that the absorbance lag may be 5–10 ps longer in pyridine than toluene. These differences in rates await further explanation.

To summarize, there are two very important points to be made from the data for NiOEP in pyridine. Further support has been provided for the $^3B_{1g}$ deactivation route and, thus, for rule (1) Second, there is strong evidence that ligands have been picked up in the excited state [rule (3)].

### 3.3 NiPPDME in pyridine

NiPPDME behaves differently in pyridine than does NiOEP in both the ground and excited states. The nickel in NiPPDME is more acidic than in NiOEP due to the presence of the vinyl and ester groups (fig 1 insert) and, therefore, NiPPDME forms a ground-state complex with two pyridines The B(0,0) band is shifted from 403 nm in toluene to 433 nm in pyridine (fig 1). Residual absorbance at 403 nm indicates that uncomplexed molecules are also present. This is also apparent from absorption in the Q-band region. As shown in fig 4C, the band at 555 nm is a mixture of the Q(0,0) transition of the uncomplexed species and the Q(1,0) band of the complexed molecules. The peak wavelengths are gathered in table 1. (An interesting observation is that in toluene the Q(0,0) band is stronger than the Q(1,0), while in pyridine and piperidine the reverse is true This follows from the discussion in section 1; the Q(1,0) band in the latter two solvents gains intensity through vibronic coupling with the Soret band which is at lower energy than in toluene.)

On the basis of these ground-state spectra, we estimate that 75–80% of the molecules are complexed. This means that most of the molecules have the paramagnetic, $^3B_{1g}(pyr)_2$ ground state This is unlike NiOEP in pyridine, where essentially all the molecules have the diamagnetic, $^1A_{1g}$ ground state. The ratio of complexed to uncomplexed species excited at any pump wavelength can be judged from the wavelength of maximum bleaching between 550 and 560 nm in the transient spectra at short delay times. On the discussion just presented, an absorption decrease at 550 nm results from bleaching the Q(1,0) band of complexed species (fig 4B), while an absorption decrease near 560 nm is due to bleaching the Q(0,0) band of the uncomplexed molecules (fig. 11A). Bleaching at intermediate wavelengths is indicative of pumping a mixture of $^1A_{1g}$ and $^3B_{1g}(pyr)_2$ ground states (figs. 11B and 11C).

The excited-state behavior is extremely dependent on excitation wavelength Pumping at 395 nm is expected to excite essentially only uncomplexed NiPPDME in pyridine The subsequent behavior is similar to that just discussed for NiOEP in pyridine, which has an uncomplexed ground state. The transient spectrum taken 40 ps after excitation at 395 nm (fig 11A) shows bleachings at 525 and 560 nm and absorption peaks at

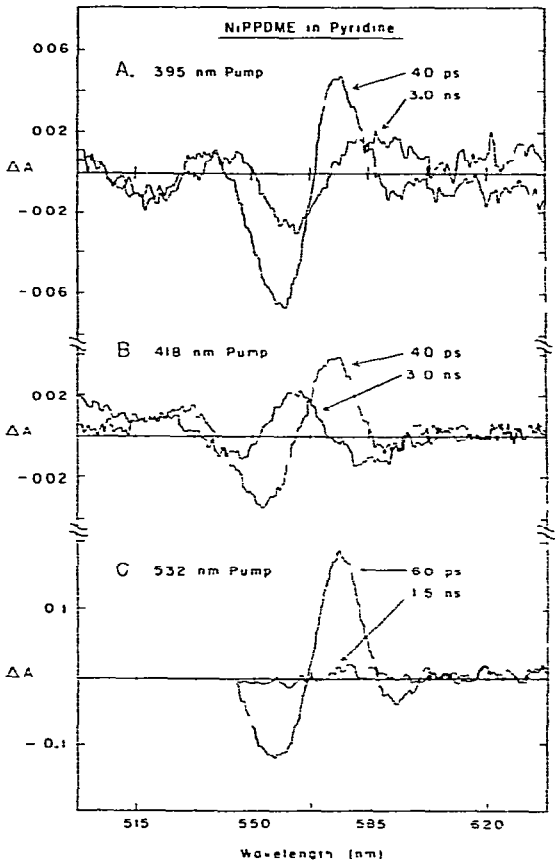


Fig 11 Transient spectra at short and long time delays following excitation of NiPPDME in pyridine at 395 nm (A) 418 nm (B) and at 532 (nm)(C) Note the similarities in the spectra at 40 60 ps delays but the dramatic differences in the behavior at longer times

nearly the same wavelengths as those found in toluene (see fig 4A) Thus, we ascribe the 40 ps spectrum in pyridine to $^3B_{1g}$. This transient absorption gives way with 450 ± 50 ps kinetics to a red-shifted long-lived state (> 20 ns lifetime) having transient absorption peaks (fig. 11A) at the same wavelengths as the ground-state Q-bands in piperidine (fig. 4C). Based on the partial ground-state recovery, the quantum yield of this state is probably 40–50%. As for NiOEP in pyridine, this suggests that $^3B_{1g}$ decays by deactivation to $^1A_{1g}$ and by picking up two pyridines to give $^3B_{1g}(pyr)_2$ These pathways are shown in fig. 12A.

The situation is different with 445 nm excitation

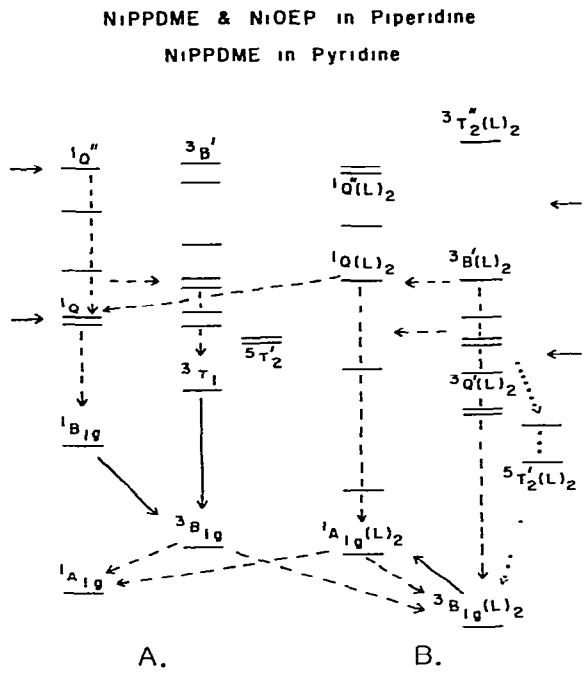


Fig 12 Summary of the photophysical and photochemical processes for NiPPDME in pyridine and for NiPPDME and NiOEP in piperidine The ordering of the states should be the same for all three cases but the energy gap between $^1A_{1g}$ and $^3B_{1g}(L)_2$ should be the most negative for NiPPDME in piperidine and the least negative for NiOEP in piperidine Based on the amount of complexation in the ground state judged from the absorption spectra, this energy gap is probably in the range $-200$ to $-800$ cm$^{-1}$. As shown, both ligand binding and release is observed in the excited-state manifold The $^3B_{1g}$ lifetime is $\approx$450 ps, while conversion of $^1A_{1g}$ to $^3B_{1g}(L)_2$ takes $>$ 20 ns For clarity, not all of the states are labeled here, but are shown in fig 2

flashes, which pump essentially only complexed molecules with a $^3B_{1g}(pyr)_2$ ground state (fig. 12B). The spectrum 40 ps after excitation (fig 4B) shows bleaching at 550 and 590 nm, and absorption peaks at the wavelengths assigned to $^3B_{1g}$ (see toluene spectrum in fig. 4A). This gives way with a time constant of 300–500 ps to a long-lived state, but in this case it is shifted to shorter wavelengths rather than to longer ones. This transient has a lifetime of $>$ 20 ns. There is significant ground-state recovery during its formation (fig. 4B). The difference spectrum of the long-lived state, shown 3 ns after excitation in fig. 4B, is very similar to the spectrum of the uncomplexed, $^1A_{1g}$ ground state in toluene; compare it with the ground-state bleaching of the transient spectrum in toluene 40 ps after excitation (fig 4A) and the ground-state spectrum in toluene (fig 4C). This observation strongly suggests that two pyridines have been ejected during the excited-state relaxation of NiPPDME in this solvent (As shown in fig. 12 and discussed in detail below, there are several routes to $^1A_{1g}$ following excitation of complexed molecules. The data just presented supports the paths through $^3B_{1g}$ ) The 40 ps spectrum of fig 4B has some absorbance at the wavelength of the absorption maximum in the 3 ns spectrum This observation is evidence for the route $^1A_{1g}(pyr)_2 \rightarrow {}^1A_{1g}$ shown in fig 12, which bypasses $^3B_{1g}$ This pathway for relaxation of complexed molecules is expected to take less than 15 ps

Further support for the decay pathways illustrated in fig. 12 comes from measurements with excitation wavelengths where both complexed and uncomplexed molecules absorb The transient behavior following excitation at 418 nm (fig. 11B) is similar to that observed with 445 nm flashes (fig. 4B) The spectrum 40 ps after excitation is assigned to $^3B_{1g}$. This state is produced by radiationless decay following excitation of uncomplexed molecules (fig. 12A) as occurs in toluene, and by ligand ejection and deactivation following excitation of complexed molecules (fig 12B). As discussed previously, $^3B_{1g}$ disappears in 450 ps by decay to $^1A_{1g}$ and to $^3B_{1g}(pyr)_2$ by binding two ligands. $^1A_{1g}$ can also be produced by other ligand ejection pathways (fig. 12). The net effect is the formation of a long-lived $^1A_{1g}$ transient absorption, shown 3 ns after the flash in fig. 11B. Re-establishment of the $^1A_{1g} \rightleftharpoons {}^3B_{1g}(pyr)_2$ ground-state equilibrium takes $>$ 20 ns to complete

Excitation of NiPPDME in pyridine with the stronger 532 nm flashes pumps a more equal mixture of complexed [$^3B_{1g}(pyr)_2$] and uncomplexed ($^1A_{1g}$) ground-state molecules. As shown in fig. 11C, the transient 60 ps after excitation is the same as that observed at 40–60 ps delays in pyridine (figs. 11A, 11B, and 4B) and in toluene (fig. 4A) It is assigned to $^3B_{1g}$ However, in this case both the transient absorbance and ground-state bleaching *completely* recover (fig 11C) with a 450 $\pm$ 35 ps time constant (figs. 9B and 9C) No long-lived component is observed. This suggests that the net result of excitation at 532 nm is the return of molecules to both uncomplexed and complexed ground states in a ratio similar to that originally pumped

Thus, we note a striking effect of excitation wave-

lengths on the transient spectra for NiPPDME in pyridine (figs 4B and 11). A similar spectrum is observed at early delays after excitation. The major features are attributable to $^3B_{1g}$ In some cases weak absorption in the $^1A_{1g}$ region is observed. This transient absorption then gives way with a 400–500 ps time constant to either a red-shifted spectrum representative of net ligand binding (fig 11A), a blue-shifted spectrum due to net ligand release (fig 4B and 11B), or no long-lived component at all (fig 11C).

A more detailed analysis of these observations and interpretations is in order. The result of pumping uncomplexed species is the disruption of the original ground-state equilibrium by the *net* conversion of some molecules from $^1A_{1g}$ to $^3B_{1g}(pyr)_2$. Different behavior occurs with excitation flashes absorbed by the complexed species. As shown in fig 12B, molecules with $^3B_{1g}(pyr)_2$ ground-states are pumped into the upper manifold of complexed triplet states Examination of table 2, fig. 2, and the work of Ake and Gouterman [12], indicates that flashes in the blue connect ground-state $^3B_{1g}(pyr)_2$ with the $^3B'(pyr)_2$, and $^3T''_1(pyr)_2$ levels, with the former carrying $\approx 100$ times the oscillator strength of the latter. Flashes in the green pump $^3B_{1g}(pyr)_2$ to the $^3T_2(pyr)_2$, $^3T'_2(pyr)_2$ and $^3Q'(pyr)_2$ manifold. The extinction coefficient of $^3Q'(pyr)_2$ should be 100 times stronger than the other two The subsequent fate of each initially populated level (figs. 2B and 12B) is determined by the relative rates with which each relaxes to a lower state [rule (1)], ejects ligands [rule (2)], or retains them [rule (3)]. As discussed previously, states with nickel $^1A_{1g}$ character should have a tendency to eject ligands These include all the states of table 1 in the column headed $^1A_{1g}$. They are, from higher to lower energy, $^1B(L)_2$, $^1Q(L)_2$, $^3T_1(L)_2$, $^3T_2(L)_2$, and $^1A_{1g}(L)_2$ (Here L = pyr) States with nickel $^1B_{1g}$ or $^3B_{1g}$ character will have a tendency to pick up ligands, or retain them in this case. These are listed in the last two columns of table 1 and are denoted with primes or double primes, respectively.

Internal conversion within the highly dense upper triplet manifold is expected to be fast (fig. 12B) This fact along with conversion to two low-lying quintets should provide an effective pathway for radiationless decay to the ground state (table 1 and fig 12) None of these states, except $^3T_2(pyr)_2$ and $^3T_1(pyr)_2$ should release their ligands. We estimate that at least 25% of the complexed molecules that are pumped return to the $^3B_{1g}(pyr)_2$ ground state in $\leqslant 15$ ps. This is based on the observation of weaker transient absorption spectra for NiPPDME in pyridine and piperidine and for NiOEP in piperidine than in the other systems. The effect cannot be explained on the basis of weaker ground-state absorption Intersystem crossing to the upper singlet manifold of complexed states (fig 12) should be favorable also due to the mixing between nickel and porphyrin states discussed above. Some of the molecules that have intersystem crossed to $^1T'_2(pyr)_2$ or $^1T'_1(pyr)_2$ probably relax rapidly back to $^3B_{1g}(pyr)_2$. Part of this decay may proceed through $^1B_{1g}(pyr)_2$.

Our observations indicate that release of ligands by complexed excited states eventually leads to the formation of $^1A_{1g}$ There appear to be several routes to this state. (Obviously, any uncomplexed molecules which are excited along with the complexed ones will deactivate through $^3B_{1g}$ to both $^1A_{1g}$ and $^3B_{1g}(pyr)_2$ )

One route into the uncomplexed manifold is due to ligand ejection in an excited state in the complexed manifold that is *above* $^3B_{1g}$ in energy. On our previous discussion and rule (2), the most likely candidates (figs 2 and 12B) are $^1Q(pyr)_2$, $^3T_1(pyr)_2$, and $^3T_2(pyr)_2$ Dissociation of ligands from these states would give the analogous states in the uncomplexed manifold, followed by rapid ($\leqslant 10$ ps) radiationless decay to $^3B_{1g}$. This gives way to $^1A_{1g}$ and through ligand binding to $^3B_{1g}(pyr)_2$ in 450 ps The observation of the same rate for NiPPDME in pyridine and for NiOEP in pyridine gives further support to this hypothesis The results also indicate that there is at least one other route to $^1A_{1g}$ that does not go through $^3B_{1g}$ Those $^1Q(pyr)_2$ that do not eject ligands (fig 12B) will deactivate to $^1A_{1g}(pyr)_2$ which being lower in energy than $^3B_{1g}$, will release two pyridines to give $^1A_{1g}$ directly. The deactivation $^1A_{1g}(pyr)_2 \rightarrow {}^3B_{1g}(pyr)_2$ may occur to some extent also, but should be slower than ligand release It should be noted that this route through $^1Q(pyr)_2$ is not accessible with excitation flashes that will not pump molecules high enough into the upper manifold of complexed triplets (figs 2B and 12B) This effect may at least partially be responsible for the observation of no long-lived component following excitation of NiPPDME in pyridine with 532 nm flashes. The accessibility of the various routes of deactivation of excited complexed molecules will be discussed further along with the results in piperidine

Let us briefly summarize this discussion of the diversity of results for NiPPDME in pyridine. Excitation of uncomplexed molecules is followed by deactivation to $^3B_{1g}$. Subsequently, molecules in this state either deactivate back to the $^1A_{1g}$ ground state or bind two pyridines to give $^3B_{1g}(pyr)_2$. The absorption spectrum at long times is red-shifted from the one at short delays. This behavior is similar to that found for NiOEP in pyridine. Excitation of complexed species, or a mixture of the two that is weighted toward complexed molecules, leads to a net conversion of $^3B_{1g}(pyr)_2$ to $^1A_{1g}$ ground states, although both ligand binding and ligand release in the excited-state manifold occur. The absorption spectra taken at long times are blue-shifted from those at short delays. The two effects balance each other following excitation in the Q-band region with 532 nm flashes which pump a more equal mixture of the two ground states. The spectrum at an early delay, having the same features as those obtained at the other pump wavelengths, decays completely in 450 ps. There is no long-lived state with the $>20$ ns time constant taken in the other cases as requisite for re-establishment of the ground-state equilibrium by either binding or release of pyridines.

### *3.4 NiOEP and NiPPDME in piperidine*

Piperidine is more nucleophilic than pyridine. Both NiOEP and NiPPDME form complexes with two piperidines to give a $^3B_{1g}(pip)_2$ ground state. We estimate the residual amount of uncomplexed molecules in the $^1A_{1g}$ ground-state to be $\approx$25% or 5–10% for NiOEP or NiPPDME, respectively. The ordering of the states shown in fig. 12B should be the same for both porphyrins. $^1B_{1g}(pip)_2$ and $^3B_{1g}(pip)_2$ should be lower and $^1A_{1g}(pip)_2$ higher in energy for NiPPDME than for NiOEP, since the former has a greater affinity for basic ligands than the latter. That NiPPDME has a higher equilibrium constant for complex formation in the ground state is consistent with previous work [2,3] and is borne out by the picosecond data. These differences do not appear to affect the general conclusions drawn from our observations in piperidine, for both porphyrins the behavior is dominated by ligand release in the excited state. At all wavelengths of excitation employed, a long-lived state is observed that has a lifetime of $>20$ ns. As shown 3 ns after excitation in figs. 3A and 4A, the absorption peaks of this metastable state are at the same wavelengths as the $^1A_{1g}$ ground state of the uncomplexed molecules. This fact is apparent upon comparison with the bleachings in the difference spectra in toluene (figs. 3A and 4A) and the ground-state absorption spectra in toluene (figs. 3C and 4C). This result is similar to that for NiPPDME in pyridine following excitation at wavelengths where complexed molecules absorb (figs. 4B and 11B). It is also in agreement with the findings of Chirvonyi et al. [12] for Ni-deuteroporphyrin IX dimethylester in piperidine.

For NiOEP or NiPPDME in piperidine *none* of the excitation wavelengths gave a long-lived state indicating *net* ligand binding in the excited state. This is due mainly to the strong affinity of these nickel porphyrins for basic ligands in the ground state. In addition, none of the pump flashes employed in the violet-blue region of the spectrum (355, 384, 395, 418 and 445 nm) is at a wavelength where absorption from the complexed B(0,0) or B(1,0) in piperidine does not dominate. (For NiPPDME in pyridine, 395 nm excitation flashes led to the observation of the net binding of ligands in the excited state because uncomplexed species are selectively pumped at this wavelength.)

The spectrum measured 40 ps after excitation at 445 nm of NiPPDME in piperidine has already developed strong characteristics of $^1A_{1g}$ (fig. 4A). This observation is markedly different from that in pyridine following excitation at the same wavelength, where the initial spectrum was found to be due mainly to $^3B_{1g}$ (fig. 4B). Assuming that mainly complexed molecules are excited at this wavelength in either solvent, and that the 445 nm flashes are energetic enough to produce a state that can intersystem cross to state $^1Q(L)_2$, then the difference in the initial spectra with basic solvent can be explained by change in the branching ratio of the routes for disappearance of this state (fig. 12). The stronger basic ligand piperidine is more tightly bound than pyridine so most of the $^1Q(pip)_2$ state radiationless decays to $^1A_{1g}(pip)_2$ rather than ejecting ligands. The step $^1A_{1g}(pip)_2 \rightarrow {}^1A_{1g}$, being much faster [rule (2)] than intersystem crossing to $^3B_{1g}(pip)_2$, is the major pathway into the uncomplexed manifold in this case. This route bypasses $^3B_{1g}$. Thus, the initial spectrum following excitation of complexed NiPPDME in piperidine is due mainly to $^1A_{1g}$ (fig. 4A). The same observation is made for NiOEP following excitation at 418 nm (fig. 3A). On the other hand, release of the less basic ligands by $^1Q(pyr)_2$ in pyridine competes favorably (fig. 12) with radiationless decay to $^1A_{1g}(pyr)_2$. As discussed previously, this path into the uncomplex-

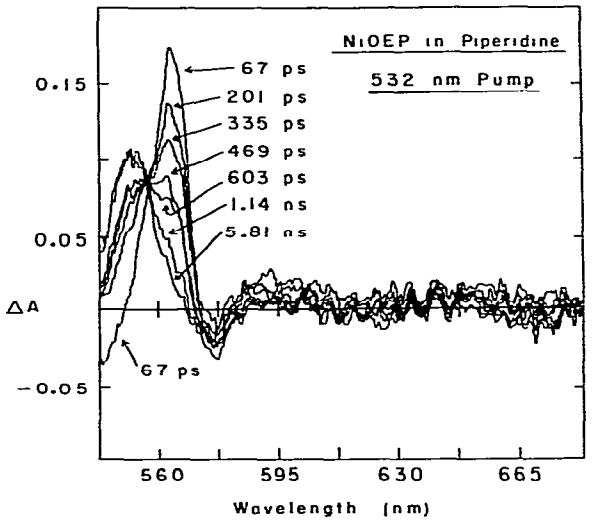


Fig 13 Evolution of the transient absorption spectra as a function of time for NiOEP in piperidine following excitation at 532 nm The decay of the transient absorption at 565 nm and the growth of that at 553 nm is clearly seen. The time constant for both processes is 450 ± 50 ps The magnitude of the long-wavelength transient absorption peak at short delays is strongly dependent on excitation wavelength for both NiOEP and NiPPDME For example, compare the spectra in piperidine for NiOEP in this figure with those of fig 3A

ed manifold leads to rapid formation of $^3B_{1g}$, the spectrum of which is shown 40 ps after excitation in fig 4B

With the exception of the results shown in fig. 12, the only indication of a state other than $^1A_{1g}$ in the spectra at early delay times in piperidine is the shoulder on the long-wavelength sides of the visible transient absorption bands (fig. 3A and 4A). On the basis of all previous discussions we attribute this spectral feature to $^3B_{1g}$ The three likely routes by which this small amount of $^3B_{1g}$ is generated are: (1) some release of piperidine from $^1Q(pip)_2$, (2) pumping some residual uncomplexed molecules and (3) loss of ligands from either $^3T_1(pip_2)$ or $^3T_2(pip_2)$. The fact that more of the $^3B_{1g}$ state is seen in the spectra at early delays following excitation with the stronger 532 nm flashes is probably due to the excitation of some uncomplexed molecules. These data are not presented for NiPPDME but is clearly seen for NiOEP in the spectra of fig. 13. The initial spectrum, which has absorption peaks at the wavelengths attributed to $^3B_{1g}$ in toluene (fig 3A), gives way to the longer-lived $^1A_{1g}$ absorption at shorter wavelengths with a time constant of 450 ± 50 ps. The finding of a similar time constant in piperidine and for those discussed above for both porphyrins in pyridine, suggests that the same state, namely $^3B_{1g}$, is largely responsible for the decay in all these cases. As shown in fig 13, conversion of the $^3B_{1g}$ Q(0,0) band to that of $^1A_{1g}$ gives rise to an isosbestic point at 558 nm, indicating that no other metastable state is involved in the transformation Any prior formation in ≤ 15 ps of some $^1A_{1g}$ by release of piperidines from $^1A_{1g}(pip)_2$ should not affect this observation

Let us summarize the results for NiOEP and NiPPDME in piperidine (fig. 12). They are dominated by release of ligands in the excited state Excitation of the small number of uncomplexed molecules with $^1A_{1g}$ ground states gives behavior similar to that for NiOEP in pyridine rapid intersystem crossing and deactivation to $^3B_{1g}$ [rule (1)] which decays by both recovery to $^1A_{1g}$ and the binding of ligands [rule (3)] to give $^3B_{1g}(pip)_2$. Excitation of the larger number of molecules with complexed, $^3B_{1g}(pip)_2$, ground states leads mainly to $^1A_{1g}$ through ligand ejection [rule (2)] via the step $^1A_{1g}(pip)_2 \rightarrow {}^1A_{1g}$. The state $^1A_{1g}(pip)_2$ is formed by deactivation of $^1Q(pip)_2$ or from lower singlets reached by pumping lower in the triplet manifold. Some $^1Q(pip)_2$ may also eject ligands The overall result is an exchange of molecules between the $^1A_{1g}$ and $^3B_{1g}(pip)_2$ ground states, with a net increase on the side of $^1A_{1g}$ The decay of this state and re-establishment of the ground state equilibrium must proceed over an activation barrier and takes > 20 ns to complete. As in the case of NiPPDME in pyridine, ≈ 30% of the initially excited complexed molecules appear to decay rapidly (≤ 15 ps) back to the ground state before any of these other processes can occur. Internal conversion in the triplet manifold appears to be rapid for all of the nickel porphyrins investigated.

## 4. Conclusions

We have reported a variety of photophysical and photochemical behavior for the nickel porphyrins. Two porphyrins, three solvents and excitation flashes at six different wavelengths between 355 and 532 nm were employed Comparison of the results under the various conditions has been helpful for attempting to understand the observations on any one of them. We have developed a set of "rules" that gives a consistent view of our results on nickel porphyrins, as well as

those of previous investigators. These concepts may be applicable also to other transition-metal porphyrins exhibiting low-lying states containing a strong metal contribution They may be particularly relevant to photodissociation and recombination of CO and $O_2$ with heme proteins

The general conclusions are: (1) Intersystem crossing and rapid relaxation to the lowest "metal" state is rapid. These processes are facilitated by mixing of porphyrin and metal configurations (2) Ligands are released by excited states with nickel $^1A_{1g}(d_{z^2})$ character. This is usually observed from the $^1Q(L)_2$ and $^1A_{1g}(L)_2$ excited states. (3) Basic ligands are bound by excited states with $^1B_{1g}$ or $^3B_{1g}(d_{z^2}, d_{x^2-y^2})$ character Ligands are picked up mainly from the low-lying $^3B_{1g}$ state The relative rates and yields of each process is determined by the particular combination of porphyrin, solvent, and excitation wavelength.

We hope our results will prompt further time-resolved investigations on transition-metal porphyrins and that the results will be helpful in understanding, on a molecular level, how metalloporphyrins function in a number of important biological systems Additional studies based on this goal are currently underway in our laboratory

### Acknowledgement

Acknowledgement is made to the donors of the Petroleum Research Fund, administered by the American Chemical Society, for partial support of this research (Grant #12798-G6) Funds were also provided by a Camille and Henry Dreyfus Foundation Grant for Newly Appointed Young Faculty in Chemistry to DH. The authors wish to thank Dr. Martin Gouterman for many helpful suggestions and stimulating discussions.

## References

[1] M. Gouterman, in The porphyrins, Vol 3, ed D Dolphin (Academic Press, New York, 1978) ch. 1, p 1
[2] B D. McLees and W S Caughey, Biochemistry 7 (1968) 642.
[3] W.S. Caughey, W.Y. Fujimoto and B P. Johnson, Biochemistry 5 (1966) 3830.
[4] W.S. Caughey and W.S Koski, Biochemistry 1 (1962) 923.
[5] R J. Abraham and P.F Swinton, J. Chem Soc II (1969) 903.
[6] G N. LaMar and F A Walker, in: The porphyrins, Vol 4 ed. D. Dolphin (Academic Press New York, 1978) p 61.
[7] R.H. Felton, in: The porphyrins, Vol 5, ed D. Dolphin (Academic Press New York, 1978) p 53
[8] E C. Johnson T. Niem and D. Dolphin, Can J Chem. 56 (1978) 1381
[9] D Dolphin and R H Felton, Accounts Chem Res 7 (1974) 26
[10] T Kobayashi, K D. Straub and P M Rentzepis, Photochem. Photobiol 29 (1979) 925
[11] V S Chirvonyi, B M. Dzhagarov, Yu.V. Timinskii and G P. Gurinovich Chem. Phys Letters 70 (1980) 79
[12] V.S Chirvonyi B M. Dzhagarov, A M Shul'ga and G P. Gurinovich, Dokl. Akad Nauka SSSR 259 (1981) 144
[13] D Eastwood and M Gouterman, J Mol Spectry 35 (1970) 359
[14] M. Gouterman, J Chem. Phys 30 (1959) 1193
[15] M Gouterman, J Mol Spectry 6 (1961) 138
[16] M Gouterman and G H Wagnière, J Mol Spectry 11 (1963) 108
[17] M H Perrin, M Gouterman and C L Perrin, J. Chem Phys 50 (1969) 4137
[18] R L Fulton and M Gouterman, J Chem Phys 41 (1961) 1059
[19] R L Ake and M. Gouterman, Theoret. Chim Acta 17 (1970) 408
[20] E.W. Baker, M S Brookhart and A H Corwin J Am Chem Soc. 86 (1964) 4587.
[21] L Saccon, in: Advances in inorganic chemistry and radiochemistry, Vol 4, eds H J Emeleus and A G Sharpe (Academic Press, New York, 1962) p 219
[22] F.A Walker and M. Bensen, J. Am Chem Soc 102 (1980) 5530.
[23] B R Henry and W. Siebrand, in: Organic molecular photophysics, Vol. 1, ed. J.B. Birks (Wiley, New York 1973) p 153
[24] D Holten, D.A. Cremers, S C Pyke, R Selensky, S S Shah, D.W. Warner and M W. Windsor, Rev. Sci Instr 50 (1979) 1653
[26] D Holten and M.W Windsor, Photobiochem Photobiophys 1 (1980) 243.
[26] N Serpone, T L Netzel and M Gouterman, J Am Chem Soc 104 (1982) 246
[27] P.A Cornelius, A W Steele, D.A. Chernoff and R M Hochstrasser, Chem Phys Letters 82 (1981) 9
[28] G A Crosby, Accounts Chem Res 8 (1975) 231
[29] D Madge and M W Windsor, Chem Phys Letters 24 (1974) 144.
[30] D. Madge, M W Windsor, D Holten and M Gouterman, Chem Phys Letters 29 (1974) 183.
[31] L. Pekkarinen and H Linschitz, J. Am Chem. Soc. 82 (1960) 2407.
[32] D Holten, M Gouterman, W W. Parson, M W Windsor and M G. Rockley, Photochem Photobiol 23 (1976) 415.
[33] J S Connolly, D S Gorman and G R Seeley, Ann NY Acad Sci 206 (1973) 649